Self-consistent level broadening in thin films with volume and surface roughness scattering

1995 J. Phys.: Condens. Matter 7 5209

(http://iopscience.iop.org/0953-8984/7/27/008)

J. Phys.: Condens. Matter 7 (1995) 5209–5228. Printed in the UK

Self-consistent level broadening in thin films with volume and surface roughness scattering

Andreas Knäbchen†

University of Technology Chemnitz-Zwickau, Institute for Physics, D-09107 Chemnitz, Germany

Received 16 February 1995

Abstract. We study the subband structure in a rough film with volume as well as surface scatterers. While volume scattering leads to an attenuation term in the differential equation of the Green function, surface roughness is incorporated via a corresponding boundary condition. The boundary condition yields a complicated behaviour of the lateral modes, e.g. complex eigenvalues and a shift of the subband thresholds, but the resulting Green function is diagonal in a lateral mode representation. In this sense, our approach contrasts with the usual perturbational treatment of surface roughness. The scattering processes give rise to intersubband transitions into both the propagating and evanescent modes. The corresponding transition rates and the scattering-induced level broadening are determined self-consistently. The thickness dependence of the density of states and of the conductivity are discussed and compared with results which follow from the neglect of level broadening. For typical parameters, level broadening along with different shifts of the subband thresholds due to various kinds of surface scatterer strongly smear out the quantum size-induced oscillations of the conductivity and the density of states. These results are in agreement with the general trend in experimental observations.

1. Introduction

The confinement of electrons in thin films gives rise to the formation of lateral subbands. Two types of these discrete levels are distinguished. The levels above the Fermi energy, infinite in number, are denoted as evanescent ones because of the exponential drop of their wavefunctions. The levels below the Fermi energy are conducting. The number of these subbands, n_c, in a smooth metallic film is given by $\mathrm{int}[k_F d/\pi]$, where k_F is the Fermi wave number and d the thickness. This implies that as d increases by half the Fermi wavelength a further subband drops below the Fermi energy and becomes conducting. According to present theoretical models, e.g. [1, 2], this interrelation between d and n_c should finally lead to pronounced periodic oscillations of physical quantities with varying thickness. The occurrence of discrete subbands and, in a narrower sense, the oscillatory behaviour just mentioned are referred to as quantum size effects (QSE). So, the lateral subbands themselves constitute an essential part of each quantum mechanical description of thin films.

In general, a real sample is neither bounded by a smooth surface nor free from volume defects. This means that we have to take into account surface-roughness-induced as well as volume scattering processes. Two consequences arise. On the one hand, scattering causes transitions between all propagating and evanescent subbands which will be characterized, in our approach, by damping quantities. The transitions are weighted by the densities of states (DOS) of the final subbands. The calculation of the damping

† Present address: Weizmann Institute of Science, Department of Condensed Matter Physics, 76100 Rehovot, Israel.

0953-8984/95/275209+20$19.50

quantities thus requires a knowledge of the DOS of all modes or, equivalently, the one-particle Green function from which the DOS can be obtained. On the other hand, the Green function itself, most conveniently expressed in a lateral mode representation, is influenced by scattering processes. In this sense, both the formation of lateral subbands and their mutual coupling are subject to scattering-induced effects, i.e. the broadening of the individual levels as well as the damping quantities (or intersubband transition rates) have to be determined self-consistently.

In a recent paper [3], we have discussed the self-consistent level broadening due to volume scattering and the corresponding DOS and electrical conductivity. It is the purpose of the present work to generalize our theory by including surface roughness scattering. In [3] the self-consistency is achieved by two equations, namely the wave equation for the Green function, G, and an optical theorem. The wave equation comprises an attenuation term, which is entirely due to the volume scatterers, while the optical theorem relates this term to the local DOS following essentially from the imaginary part of G. To incorporate surface roughness, we proceed in a similar way. In particular, the properties of the rough surface profile are described in terms of surface scatterers. One can associate these scatterers with isolated bumps and dips on the surface. (The mathematical formulation of surface scattering can be found in [4–6].) A corresponding optical theorem for the surface scatterers holds, too, whereas the differential equation for G remains unchanged. However, instead of the hard-wall boundary condition, we are guided to a complex boundary condition imposed on the lateral modes. Some interesting effects follow directly from the boundary condition that itself represents an essential result. For instance, the intersubband damping quantity does not increase monotonically with the subband index but saturates. In addition, the subband thresholds are shifted towards higher or lower energies.

The self-consistent level broadening leads to further modifications of the resulting quantities. So, for instance, level broadening reduces considerably the QSE oscillations. It is well known that there is a significant deviation between the amplitudes of these oscillations predicted by current theories and the measured ones [7–11]. Therefore, we argue that scattering-induced level broadening may, at least partly, account for this discrepancy. Hence, the theory of level broadening along with the effects resulting from the new boundary condition just mentioned can contribute to a deeper general understanding of the QSE.

If we neglect the level broadening processes, and consider the propagating modes only, we reach the case normally studied in analytical descriptions of the electrical conductivity in thin films [12–14, 1, 2, 15, 6, 16]. Assuming, moreover, a simple limiting behaviour of the roughness-induced damping to be approximately valid for all conducting subbands, our approach reproduces some formulae for the conductivity derived previously in the framework of a perturbational treatment of surface roughness. For instance, we confirm the well known results obtained by Trivedi and Ashcroft [1] and Fishman and Calecki [2]. So, in some respects, their discussions of the fit of conductivity measurements by the theoretical expressions are also accurate here and thus do not need to be repeated.

The formalism we use is called the superposition method (SPM). We have shown that the SPM, also in its lowest approximation, is well suited to treat d.c. transport in problems with spatial restrictions [17–19, 6]. The main assumption of the SPM as applied in this paper concerns the neglect of higher-order quantum corrections to the density matrix [20], which is justified for sufficiently weak scattering processes. This implies that, e.g. with respect to volume scattering, the mean free path l within the ensemble of disordered background scatterers is large compared with the Fermi wavelength. For good bulk conductors, e.g. metals, the smallness of the parameter $(lk_F)^{-1}$ is fulfilled.

The SPM can be applied to the diffusion case with a given gradient of the chemical

potential or to the mobility case with a driving force [20]. The diffusion case is mathematically much simpler than the force case and therefore we choose it to start with. This decision is only a formal matter because it is well known how to transform the results into the force picture via the Einstein equivalence.

Our paper is organized as follows. In the next section we derive the boundary condition mentioned above and find the general form of the Green function. Furthermore, the optical theorems for both volume and surface scatterers are introduced. The DOS is a quantity which follows immediately from the Green function and is therefore given in section 3. In section 4, we outline the basic formulae of the SPM and apply them to the layer system under consideration. This yields a formula for the electrical conductivity σ. In section 5 we study in detail the wave numbers μ_n^2 associated with the in-plane propagation process. Since volume and surface scattering contribute individual terms to μ_n^2 they are discussed separately. In section 6 we summarize at first some approximate expressions for σ following from the neglect of level broadening and with further assumptions as mentioned above. Then, we illustrate the exact results for the DOS and the conductivity by a series of figures and confront them with the approximate solutions derived in previous parts of this work. Finally, a summary is given in section 7.

2. Green function

One of the basic ingredients of the SPM is the one-particle Green function, averaged over all configurations of volume and surface scatterers, respectively. The Green function describes completely the propagation and scattering-induced attenuation of a coherent electron wave and obeys the equation [6]

$$G(\boldsymbol{r},\boldsymbol{r}') = G_0(\boldsymbol{r},\boldsymbol{r}') + \int \mathrm{d}^3\boldsymbol{r}''\, \mathcal{N}_v\, G_0(\boldsymbol{r},\boldsymbol{r}'') 4\pi \tilde{f}_v(z'') G(\boldsymbol{r}'',\boldsymbol{r}') + \int_{z''=\pm a} \mathrm{d}^2\boldsymbol{R}''\, \mathcal{N}_s\, k_0^{-2} \frac{\partial}{\partial z''} G_0(\boldsymbol{r},\boldsymbol{r}'') 4\pi \tilde{f}_s \frac{\partial}{\partial z''} G(\boldsymbol{r}'',\boldsymbol{r}') \tag{1}$$

where we have employed cylindrical co-ordinates $\boldsymbol{r} = (\boldsymbol{R}, z)$; the z axis is orientated perpendicularly to the surfaces which are located at $z = \pm a$ (thickness $d \equiv 2a$). The vacuum propagator for the layer geometry is denoted by G_0; k_0 is the corresponding wave number. The scatterers are homogeneously distributed with mean density $\mathcal{N}_v$ within the film, and with mean areal density $\mathcal{N}_s$ on the surfaces, respectively. For the sake of brevity, we have assumed that *both* surfaces are covered equally with scatterers. The transition to a layer with two different lateral boundaries is straightforward. $\tilde{f}_v(z)$, $\tilde{f}_s$ are the corresponding scattering amplitudes in which all backscattering processes with the surroundings are included, see [20]. For sufficiently weak scatterers, backscattering yields only a small renormalization of the original scattering amplitudes f_v and f_s. In particular, one can set $\mathrm{Re}\,\tilde{f} \approx \mathrm{Re}\,f$ because the small corrections to the real parts cannot compete with the particle energy ($\sim k_0^2$) that dominates the real part of the resulting wave number for G, cf (2). The imaginary parts $\mathrm{Im}\,\tilde{f}$, however, exclusively responsible for the attenuation of the Green function, require a sound consideration, cf. (5). Particularly in the vicinity of subband thresholds the quantities $\mathrm{Im}\,\tilde{f}_v(z)$, $\mathrm{Im}\,\tilde{f}_s$ may deviate considerably from their values well inside a subband.

Applying the differential operator $[\Delta + k_0^2]$ to (1), we find

$$[\Delta + k_0^2 + 4\pi \tilde{f}_v(z)\mathcal{N}_v] G(\boldsymbol{r}\boldsymbol{r}') = -\delta(\boldsymbol{r}-\boldsymbol{r}') \tag{2a}$$

$$G(\boldsymbol{r},\boldsymbol{r}')|_{z'=\pm a} = \mp \frac{4\pi \tilde{f}_s \mathcal{N}_s}{k_0^2} \frac{\partial}{\partial z'} G(\boldsymbol{r},\boldsymbol{r}')|_{z'=\pm a}\,. \tag{2b}$$

The wave equation for G follows from the volume contribution in (1), whereas the boundary condition† results from the surface term. The complex boundary condition (2*b*) is fixed by a single parameter, namely $\alpha \equiv 4\pi \tilde{f}_s \mathcal{N}_s k_0^{-2}$. For vanishing surface scattering, $\alpha = 0$, formula (2*b*) reduces to the ordinary hard-wall boundary condition. The parameter α can be easily interpreted if we model surface scatterers by small and isolated bumps or dips on the surface. From an experimental point of view, bumps and dips may be associated with surplus or missing atoms, respectively, on an otherwise atomically smooth surface layer. Guided by the analysis given in [5], one can deduce (namely from formula (8) in the cited paper) the relation

$$4\pi \operatorname{Re} f_s = k_0^2 V \tag{3}$$

which yields the dominating real part of the scattering amplitude in terms of the volume of the surface irregularities. One has $V > 0$ and $V < 0$ for bumps and dips, respectively. Substituting (3) into α, we find

$$\operatorname{Re} \alpha = \mathcal{N}_s V \tag{4}$$

i.e. $\operatorname{Re}\alpha$ corresponds to a mean deviation h in the height of the surface (or the thickness of the film). Additionally, $\operatorname{Re}\alpha$ is energy independent.

Bearing this interpretation of α in mind, the boundary condition (2*b*) is, in some respects, similar to that used as the basic *ansatz* in the perturbation method (see, for instance, [21, 22]). According to this method, the boundary condition $\Psi|_{\text{surface}} = 0$, imposed on the total wave field, can be expanded in terms of the small height deviation from the mean surface profile. Up to first order, this series expansion yields

$$\Psi(\boldsymbol{r})|_{z=\pm a} = \mp h(\boldsymbol{R}) \partial\Psi/\partial z|_{z=\pm a}.$$

In contrast to the perturbation method, however, the parameter α is a complex quantity. Its imaginary part $\sim \operatorname{Im} \tilde{f}_s$ follows from the presence of configurationally averaged surface scatterers and is associated with the loss that a coherent waveform suffers at reflection at the surface. A similar attenuation process, caused by volume scatterers, occurs within the film. Nevertheless, the total particle density is conserved because (1) optical theorems for both types of scatterer guarantee particle conservation for each individual scattering process, and (2) each scatterer acts simultaneously as a source of an emerging wave. So the superposition of all scattered waves reproduces the original wave field, cf. the construction of the density matrix (14).

The optical theorem for the volume scatterers is

$$\operatorname{Im} \tilde{f}_v(z) = 4\pi |\tilde{f}_v|^2 \operatorname{Im} G(\boldsymbol{r}, \boldsymbol{r}). \tag{5a}$$

Together with the wave equation (2*a*), this formula makes possible a self-consistent treatment of the level broadening due to volume scattering, see [3]. In order to generalize our approach to surface roughness scattering, the boundary condition (2*b*) has to be complemented by the corresponding optical theorem [5]

$$\operatorname{Im} \tilde{f}_s = 4\pi |\tilde{f}_s|^2 k_0^{-2} \frac{\partial^2}{\partial z \partial z'} \operatorname{Im} G(\boldsymbol{r}, \boldsymbol{r}')|_{\boldsymbol{r}'=\boldsymbol{r}=(\boldsymbol{R}, \pm a)} . \tag{5b}$$

† A boundary condition of this kind is sometimes referred to as the impedance boundary condition [21].

The formulae (2) and (5) represent a closed system of equations and provide a complete description of the Green function. To simplify these formulae, we introduce a lateral mode representation. Actually, $G(r, r')$ can be represented in its most general form as a double sum over all lateral modes of the film [3]. Employing similar arguments as in [17], we may restrict ourselves to the diagonal elements only because the non-diagonal ones are negligible for sufficiently weak *volume* scattering. Note that non-diagonal elements do not arise from surface scattering at all. Thus, equations (2) are formally solved by

$$G(\boldsymbol{r}, \boldsymbol{r}') = \sum_{n=1}^{\infty} \varphi_n^*(z)\varphi_n(z')G_n(\mu_n|\boldsymbol{R} - \boldsymbol{R}'|). \tag{6}$$

The term $G_n = (\mathrm{i}/4)H_0^{(1)}$ is the two-dimensional Green function and agrees, up to a factor i/4, with the Hankel function of the first kind and zeroth order [23]. The $\{\varphi_n\}$ represent a complete [24] set of normalized eigenfunctions and fulfill the equations

$$[\partial^2/\partial z^2 + \kappa_n^2]\varphi_n(z) = 0 \qquad \varphi_n(\pm a) = \mp\alpha\partial\varphi_n(z)/\partial z|_{z=\pm a}. \tag{7}$$

The wave number μ_n is given by

$$\mu_n^2 = k_0^2 - \kappa_n^2 + 4\pi(\tilde{f}_v)_n\mathcal{N}_v \tag{8}$$

with the matrix element

$$(\tilde{f}_v)_n = \int_{-a}^{a} \mathrm{d}z\, \varphi_n^*(z)\tilde{f}_v(z)\varphi_n(z). \tag{9}$$

The term $\mathrm{Re}\,\mu_n^2$ can be considered as the remaining energy for the in-plane propagation for each individual subband. Strictly speaking, only a finite number n_c of modes with $\mathrm{Re}\,\mu_n^2 > 0$ allow a real propagation process, whereas the others, due to the exponential drop of their wavefunctions, are evanescent. The term $\mathrm{Im}\,\mu_n^2$ is the characteristic damping quantity (or, except for a factor $\hbar/m$, transition rate) for each subband and results solely from the occurrence of scattering processes, i.e. $\mathrm{Im}\,\alpha > 0$ and/or $\mathrm{Im}\,(\tilde{f}_v)_n > 0$. Both volume and surface contributions to $\mathrm{Im}\,\mu_n^2$ are always non-negative, of course. Note that

$$-\mathrm{Im}\,\kappa_n^2 = 2\,\mathrm{Im}\,\alpha\,|\partial\varphi_n/\partial z|_{z=\pm a}|^2 \tag{10}$$

which follows from equations (7) guarantees $-\mathrm{Im}\,\kappa_n^2 \geqslant 0$. Thus, the real and imaginary parts of μ_n^2 determine completely the basic properties of the in-plane process. In particular, they yield the density of states (DOS), averaged over the cross-sectional coordinate z, for each individual subband, and the conductivity. Before investigating the solution of equations (7) and (8) explicitly, let us introduce the DOS as well as the conductivity.

3. Density of states

The influence of the scattering processes on the formation of the lateral subbands is conveniently expressed in terms of the DOS of each individual mode [3]. Remember that the DOS itself is directly related to the scattering amplitudes via the optical theorems (5). For completeness, we summarize in what follows some properties of the DOS which have already been discussed in more detail in [3]. The local DOS is essentially given by

the imaginary part of the Green function (6), namely $(2m/\pi\hbar^2)\mathrm{Im}\,G(\boldsymbol{r},\boldsymbol{r})$ (for one spin component only). An important and more compact quantity is the DOS averaged over the lateral coordinate z that will be used below. It reads

$$N(k_0,d) = (m/2\pi\hbar^2 d)\sum_{n=1}^{\infty} N_n \tag{11}$$

$$N_n = \Theta(\mathrm{Re}\,\mu_n^2) - \pi^{-1}\tan^{-1}(\mathrm{Im}\,\mu_n^2/\mathrm{Re}\,\mu_n^2) \tag{12}$$

where Θ is the step function. The expression (12) arises from the behaviour of the Hankel function in (6) in the limit of small arguments [23]. Formula (11) shows that all subbands contribute with their individual DOS ($\sim N_n$) to the total one. Actually, the terms of the n_c propagating modes ($\mathrm{Re}\,\mu_n^2 > 0$) are dominant, whereas the evanescent modes ($\mathrm{Re}\,\mu_n^2 < 0$) yield only small corrections for energies far from the subband thresholds. Neglecting the scattering processes, $\mathrm{Im}\,\mu_n^2 \to 0$, see below, the DOS of all propagating modes approach the maximal value, $N_n \to 1$, and the evanescent modes have zero DOS, $N_n \to 0$, i.e. no carriers are scattered in or out of these states. In this case, we obtain from formula (11) the DOS of a smooth film without scatterers:

$$N^0(k_0,d) = mn_c/2\pi\hbar^2 d. \tag{13}$$

Here, $n_c = \mathrm{int}[k_0 d/\pi]$. Hence N^0 shows the typical staircase-like behaviour of the DOS as a function of wave number. For later convenience, we introduce the size-independent local DOS of the bulk system, $N_b(k_0) = (mk_0/2\pi^2\hbar^2)$, which results from N^0 in the limit of infinite thickness d.

The simple limiting situation just discussed changes when scattering processes are taken into account. Generally, their occurrence reduces the DOS of the propagating modes but increases that of the evanescent ones. As (12) indicates, even the very existence of states in the evanescent subbands is associated with the occurrence of scattering processes, i.e. $\mathrm{Im}\,\mu_n^2 > 0$. The specific influence of these processes on the DOS depends on the in-plane energy ($\sim \mathrm{Re}\,\mu_n^2$) of each subband. In particular, the highest conducting mode ($\mathrm{Re}\,\mu_{n_c}^2 \gtrsim 0$) as well as the lowest evanescent mode ($\mathrm{Re}\,\mu_{n_c+1}^2 \lesssim 0$) are affected strongly by intersubband scattering. To ensure the convergence of the sum (11), i.e. a finite DOS, and the existence of the expressions (5), the contributions N_n of the higher non-propagating modes have to vanish in the limit $n \to \infty$, see section 5.

4. Density matrix and conductivity

The SPM rests on the idea that the density matrix $\varrho(\boldsymbol{r},\boldsymbol{r}')$ can be constructed via the superposition of waves emerging from all scatterers belonging to a given system. Here, volume as well as surface scatterers contribute to the whole wave field. Accordingly, the density matrix comprises two terms [6]

$$\varrho(\boldsymbol{r},\boldsymbol{r}') = \int \mathrm{d}^3\boldsymbol{r}''\,\mathcal{N}_v|4\pi\,\tilde{f}_v(z'')|^2\,G^*(\boldsymbol{r},\boldsymbol{r}'')G(\boldsymbol{r}',\boldsymbol{r}'')\,|\psi(\boldsymbol{r}'')|^2$$
$$+\int_{z''=\pm a}\mathrm{d}^2\boldsymbol{R}''\,\mathcal{N}_s|4\pi\,\tilde{f}_s|^2\,k_0^{-4}\frac{\partial}{\partial z''}G^*(\boldsymbol{r},\boldsymbol{r}'')\frac{\partial}{\partial z''}G(\boldsymbol{r}',\boldsymbol{r}'')\left|\frac{\partial}{\partial z''}\psi(\boldsymbol{r}'')\right|^2 \tag{14}$$

where $\psi(\boldsymbol{r})$ is the wave field at the point $\boldsymbol{r}$. Inserting the optical theorems (5) into (14), we obtain, for instance, in the volume contribution the expression $|\psi(\boldsymbol{r})|^2/\mathrm{Im}\,G(\boldsymbol{r},\boldsymbol{r})$.

The carrier density $|\psi|^2$ is given by the local DOS and the Fermi distribution function, $f(E-\mu(r))$. Furthermore, in the diffusion picture applied here, a stationary current parallel to the film surfaces is driven by a corresponding gradient of the chemical potential, $\partial\mu/\partial r = \partial\mu/\partial R = \text{constant}$. This implies

$$\frac{\partial}{\partial r}\left(\frac{|\psi(r)|^2}{\operatorname{Im} G(r,r)}\right) = \frac{2m}{\pi\hbar^2}\left(-\frac{\mathrm{d}f}{\mathrm{d}E}\right)\frac{\partial\mu}{\partial R} \equiv g = \text{constant}. \tag{15}$$

Similar considerations apply to the corresponding surface expression, see [6], leading to the relation

$$\frac{|\psi(r)|^2}{\operatorname{Im} G(r,r)} = \frac{|\frac{\partial}{\partial z}\psi(r)|_{z=\pm a}|^2}{\frac{\partial^2}{\partial z\partial z'}\operatorname{Im} G(r,r')|_{r'=r=(R,\pm a)}} = gR + C \qquad C = \text{constant}. \tag{16}$$

With the representation (6) of the Green function and the latter formula, we can write the density matrix in the form

$$\varrho(r,r') = \sum_{n=1}^{\infty}\varphi_n^*(z)\varphi_n(z')\operatorname{Im}\mu_n^2\int_{z''=\pm a}\mathrm{d}^2R''\,[gR''+C]G_n^*(\mu_n|R-R''|) \times G_n(\mu_n|R'-R''|) \tag{17}$$

where all non-diagonal elements are again neglected [17], and the integration over z'' in the first integral in formula (14) has been carried out. To combine the volume and surface damping in $\operatorname{Im}\mu_n^2$ (8), we have used the identity (10). Obviously, the density matrix (17) guarantees the aforementioned density reproduction, namely

$$\varrho(r,r) = [gR+C]\operatorname{Im} G(r,r) = |\psi(r)|^2.$$

The current density can be derived from the density matrix

$$j(r) = \frac{\hbar}{m}\operatorname{Im}\frac{\partial}{\partial r'}\varrho(r,r')|_{r'=r}. \tag{18}$$

The electrical conductivity σ is associated with the laterally averaged current density and requires the transition from the diffusion case to the more familiar force case. This transition employs essentially the Einstein equivalence between $-\partial\mu/\partial R$ and a driving force, and was discussed in our earlier papers based on the SPM [20, 19]. Here, we only give the result [3]:

$$\sigma(d) = \frac{e^2}{2\pi\hbar d}\sum_{n=1}^{\infty}\left(\frac{\operatorname{Re}\mu_n^2}{\operatorname{Im}\mu_n^2}N_n + \frac{1}{\pi}\right). \tag{19}$$

Expression (19) is valid for a degenerate electron gas, i.e. all quantities have to be taken at the Fermi energy $k_0 = k_F$. As shown in [3], formula (19) represents a natural generalization of the quasiclassical conductivity, $\sigma(d) \sim \sum_{n=1}^{n_c}\operatorname{Re}\mu_n^2/\operatorname{Im}\mu_n^2$ [1, 6] to a system where level broadening is taken into account.

5. Wave number μ_n^2

While surface roughness scattering contributes independently via κ_n^2 to μ_n^2 (8), the volume term $(\tilde{f}_v)_n$ is affected by the lateral eigenfunction φ_n which depends on the boundary condition (7) imposed. Therefore, let us first investigate the eigenfunctions and eigenvalues φ_n and κ_n, respectively, and then return to the volume contribution.

5.1. Surface contribution κ_n^2

The general solution of the differential equation (7) is given by

$$\varphi = A\exp(\mathrm{i}\kappa z) + B\exp(-\mathrm{i}\kappa z) \qquad A, B = \text{constant}.$$

Inserting this *ansatz* into the boundary condition (7), we find the two cases $A = \pm B$, corresponding to $\varphi_n \sim \sin\kappa z$ or $\cos\kappa z$, and the equations

$$\mathrm{e}^{\mathrm{i}\kappa d} = \pm\frac{1 - \mathrm{i}\kappa\alpha}{1 + \mathrm{i}\kappa\alpha} \tag{20a}$$

which yield the eigenvalues κ_n. Alternatively, these equations can be written in the form

$$\tan\kappa a = -\alpha\kappa \qquad \cot\kappa a = \alpha\kappa. \tag{20b}$$

These formulae show that the $\{\varphi_n\}$ are given by an alternating sequence of cosine and sine functions. Generally, a large number of solutions for (20*a*) or (20*b*), as necessary to evaluate the optical theorems, the DOS etc, can be calculated only numerically. It is instructive, however, to consider two analytical approximations valid in the limiting cases of $|\alpha\kappa_n| \ll 1$ or $|\alpha\kappa_n| \gg 1$, respectively. In the first case, which will be useful in estimating the lowest modes $n = 1, 2, \ldots$, we find

$$\kappa_n \approx \kappa_n^0(1 - \alpha/a) \qquad |\alpha\kappa_n| \ll 1 \tag{21}$$

where $\kappa_n^0 = (2n-1)\pi/d$ ($\kappa_n^0 = 2n\pi/d$) for $\varphi_n \sim \cos\kappa z$ ($\varphi_n \sim \sin\kappa z$). In the opposite case, which is associated with the asymptotic behaviour of the φ_n, $n \gg 1$, one obtains

$$\kappa_n \approx \kappa_n^0\left(1 + \frac{1}{a\alpha(\kappa_n^0)^2}\right) \qquad |\alpha\kappa_n| \gg 1. \tag{22}$$

Now, $\kappa_n^0 = 2n\pi/d$ ($\kappa_n^0 = (2n-1)\pi/d$) for $\varphi_n \sim \cos\kappa z$ ($\varphi_n \sim \sin\kappa z$). In the complex κ plane, the eigenvalues κ_n form initially, according to expression (21), a straight line with decreasing imaginary part for increasing n. Then, $\mathrm{Im}\,\kappa_n$ passes through a minimum. Eventually, $\mathrm{Im}\,\kappa_n$ increases so that the κ_n approach the real axis from below, see figure 1. The values of $\mathrm{Re}\,\kappa_n$ lie for small n as well as for large n in the vicinity of an integer multiple of π/d. It is worth realizing, however, that the real part of κ_n moves, for instance for $\varphi_n \sim \cos\kappa z$, from an odd multiple of π/d to an even multiple for increasing n, namely to the next larger or smaller value. The direction of this shift is determined by the sign of $\mathrm{Re}\,\alpha \sim \mathrm{Re}\,\tilde{f}_s$. For bumps/dips on the surface, $\mathrm{Re}\,\tilde{f}_s \gtrless 0$, see section 2, all $\mathrm{Re}\,\kappa_n$ are shifted to the left/right. This behaviour can be understood by bearing in mind that the appearance of surface scatterers corresponds to a mean thickness deviation $h = \mathrm{Re}\,\alpha = \mathcal{N}_s V$. Indeed, employing an effective thickness $d + 2h$ (both surfaces are covered with scatterers), the κ_n^0 (n small) are reduced/increased if $h \gtrless 0$. On principle, the behaviour of both the real and imaginary parts of the eigenvalues $\{\kappa_n\}$ is essential to obtain consistent results for all physical quantities.

In figure 1, a series of eigenvalues κ_n is shown. The shift of $\mathrm{Re}\,\kappa_n$ can be clearly seen. Note that the trivial solution $\kappa_0 = 0$ as well as a second set of eigenvalues caused by the invariance of equations (20) under $\kappa \to -\kappa$ are omitted.

The approximation (21) is not only valid for small n but also for very weak surface scattering, $\alpha \to 0$. If we neglect, with respect to the determination of the lateral

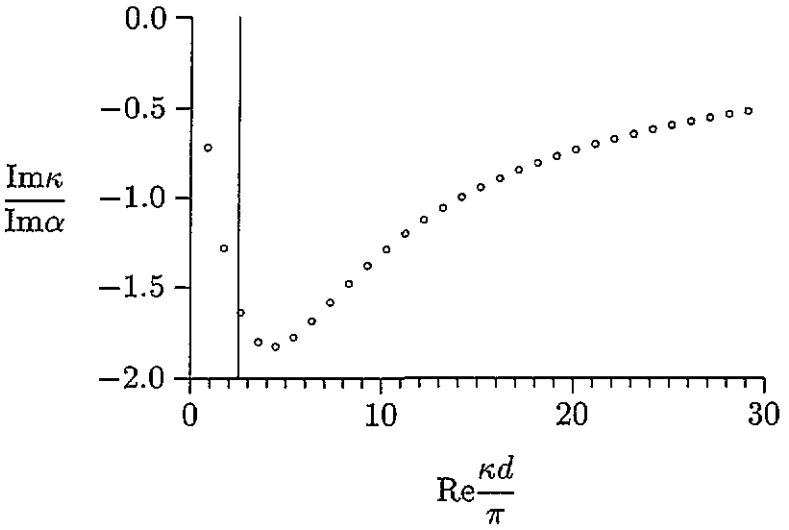

Figure 1. The lowest eigenvalues κ_n, calculated from the transcendental equations (20), are shown. The parameters are $4\pi\mathcal{N}_s|\tilde{f}_s|^2 = 0.2$, Re$\tilde{f}_s$=0.1 and $d = 2.5$ leading to a value Im $\alpha = 0.013\,62$ determined self-consistently (the latter three quantities are given in units of π/k_0). Because Re $\alpha \approx 0.2 > 0$ the eigenvalues are shifted to the left. The straight line at Re $\kappa d/\pi = 2.5$ marks the boundary between propagating and evanescent modes.

eigenfunctions, the deviation of κ_n from κ_n^0, we obtain $\varphi_n^0(z) = \sqrt{2/d}\sin\frac{n\pi}{d}(z-a)$, $n = 1, 2, \ldots$, i.e. the well known solution for hard-wall boundary conditions. In a series of papers, weak surface roughness scattering has been included via a perturbational treatment. This means that transition matrix elements have been calculated based on the unperturbed eigenfunctions φ_n^0 and an appropriately chosen roughness potential. In this sense, one may anticipate that the damping resulting from the approximation (21) is related to these transition rates. In our formalism, the roughness-induced intersubband scattering is given by $-\mathrm{Im}\,\kappa_n^2$ (cf. (8)). Using the approximate expression (21), this yields

$$-\mathrm{Im}\,\kappa_n^2 \approx \frac{16\pi^3\mathcal{N}_s}{k_0^2 d^3} n^2 \mathrm{Im}\,\tilde{f}_s. \tag{23}$$

Indeed, the explicit dependence $-\mathrm{Im}\,\kappa_n^2 \sim n^2 d^{-3}$ of this result was found by various authors (see, for instance, [1]). If we employ the optical theorem (5*b*) in an equivalent approximate form (φ_n^0 instead of φ_n)

$$\mathrm{Im}\,\tilde{f}_s \approx 4\pi|\tilde{f}_s|^2 \frac{1}{2k_0^2 d}\sum_{n=1}^{n_c}\left(\frac{n\pi}{d}\right)^2 \tag{24}$$

we find with $N_n \approx 1$ for $n \leqslant n_c$

$$-\mathrm{Im}\,\kappa_n^2 \approx \frac{32\pi^6\mathcal{N}_s|\tilde{f}_s|^2}{k_0^4 d^6} n^2 S(n_c) \qquad S(n_c) = \sum_{n=1}^{n_c} n^2 = \tfrac{1}{6}n_c(n_c+1)(2n_c+1). \tag{25}$$

This expression for the roughness-induced damping was derived by Fishman and Calecki [2] based on a geometrical roughness description and thus different parameters, and was later

confirmed by Kunze [6] employing the SPM as applied here. In deriving the latter formula we have truncated the sum (24) at $n = n_c$. Of course, this is a rather artificial step, but necessary to render the sum convergent. Indeed, the further terms are of the order of $-n^2 \mathrm{Im}\,\mu_n^2/\mathrm{Re}\,\mu_n^2 \sim \mathrm{Im}\,\mu_n^2$, i.e. they increase if the contribution $-\mathrm{Im}\,\kappa_n^2$ (23) to $\mathrm{Im}\,\mu_n^2$ is used.

Now, let us comment on the asymptotic behaviour ($|\kappa_n^0\alpha| \gg 1$) of κ_n and φ_n which removes the divergence just discussed. From the approximation (22) it follows that

$$-\mathrm{Im}\,\kappa_n^2 \approx \frac{k_0^2}{\pi \mathcal{N}_s |\tilde{f}_s|^2 d} \mathrm{Im}\,\tilde{f}_s \tag{26}$$

i.e. the roughness-induced damping saturates at a value independent of the subband index n. The ratio of the damping quantities of the lowest modes to that of the large ones is given by

$$\frac{\mathrm{Im}\,\kappa_n^2|_{n\ \mathrm{small}}}{\mathrm{Im}\,\kappa_n^2|_{n\ \mathrm{large}}} \approx (\kappa_n^0|_{n\ \mathrm{small}})^2 \mathcal{N}_s^2 V^2 \approx |\kappa_n^0|_{n\ \mathrm{small}}\alpha|^2 \ll 1. \tag{27}$$

Thus, the damping varies considerably if the lowest subbands are weakly affected by the surface roughness. The corresponding condition is $|\alpha\kappa_n^0| \approx 2\pi h/\lambda_n^0 \ll 1$, i.e. the mean deviation of the film thickness has to be small compared to the wavelength λ_n^0 that can be assigned to the individual subbands.

In the lateral mode representation, the optical theorem (5*b*) for the surface scatterers has the form

$$\mathrm{Im}\,\tilde{f}_s = \pi |\tilde{f}_s|^2 k_0^{-2} \sum_{n=1}^{\infty} N_n |\partial\varphi_n(z)/\partial z|_{z=a}|^2 = \frac{\pi |\tilde{f}_s|^2}{2k_0^2 \mathrm{Im}\,\alpha} \sum_{n=1}^{\infty} N_n(-\mathrm{Im}\,\kappa_n^2). \tag{28}$$

Since the damping quantities of the higher modes (26) remain finite, the behaviour of N_n alone determines their summands in the latter formula. Because $N_n \to -\mathrm{Im}\,\mu_n^2/\mathrm{Re}\,\mu_n^2 \sim n^{-2}$ for $n \gg n_c$, the sum (28) is now convergent without any further requirements.

5.2. *Volume contribution* $(\tilde{f}_v)_n$

For weak (volume) scattering, as discussed in section 2, the approximation $\mathrm{Re}\,\tilde{f}_v \approx \mathrm{Re}\,f_v$ is justified. Hence, the real part of the matrix element (9) is sufficiently determined by $\mathrm{Re}\,(\tilde{f}_v)_n = \mathrm{Re}\,f_v$. To calculate its imaginary part, responsible for the volume-scattering-induced intersubband transitions, the lateral dependence of $\mathrm{Im}\,\tilde{f}_v(z)$ has to be taken seriously. Substituting the optical theorem (5*a*) into (9) yields

$$\mathrm{Im}\,(\tilde{f}_v)_n = \pi |\tilde{f}_v|^2 \sum_{m=1}^{\infty} N_m \int_{-a}^{a} \mathrm{d}z\, |\varphi_n(z)|^2 |\varphi_m(z)|^2. \tag{29}$$

The integral in this equation gives a finite numerical value, so that the convergence of the sum is guaranteed 'automatically' by the vanishing DOS $\sim N_n \sim n^{-2}$ of the higher evanescent modes. The expression (29) can be readily evaluated only in the case when the influence of surface roughness on the lateral eigenfunctions is negligible, $\varphi_n \approx \varphi_n^0$, and level broadening is suppressed completely, $N_n \approx \Theta(\mathrm{Re}\,\mu_n^2)$. Then

$$4\pi \mathrm{Im}\,(\tilde{f}_v)_n \mathcal{N}_v \approx \frac{\pi}{d}(n_c + \tfrac{1}{2}) 4\pi |\tilde{f}_v|^2 \mathcal{N}_v \equiv \frac{\pi}{dl}(n_c + \tfrac{1}{2}) \qquad n \leqslant n_c. \tag{30}$$

In simplifying this expression we have invented the familiar definition of the mean free path l as the inverse product of the integral scattering cross-section, $4\pi|\tilde{f}_v|^2$, and the density of scatterers, $\mathcal{N}_v$. The damping quantity (30) is at least approximately independent of the subband index. Without level broadening, this property is in agreement with the behaviour of the two-dimensional DOS and the assumed isotropic volume scattering, of course. The (approximate) formula (30) represents the well known result for volume-scattering-induced damping, first derived by Sandomirskii [12], and confirmed later by Trivedi and Ashcroft [1]. The corrections to $\mathrm{Im}\,(\tilde{f}_v)_n$, arising from a self-consistent treatment of volume scattering processes alone, have been discussed in [3].

6. Conductivity and density of states

In the previous sections, the Green function (6) as well as the optical theorems (5) have been rewritten in a lateral mode representation. This representation makes possible an efficient self-consistent solution of these equations. As a starting *ansatz* for $\mathrm{Im}\,(\tilde{f}_v)_n$ and $\mathrm{Im}\,\tilde{f}_s$, the approximate expressions (30) and (24), respectively, can be used. The corresponding numerical results will discussed in the second part of this section. Before this, let us determine the properties of the conductivity following from the neglect of self-consistent level broadening. (In the case of negligible level broadening, the averaged DOS N (11) reduces to N^0 (13) and thus requires no further comment.)

6.1. Approximate formulae for σ

Without level broadening, the conductivity of a degenerate electron gas ($k_0 = k_F$) is given by

$$\sigma(d) = \frac{e^2}{2\pi\hbar d}\sum_{n=1}^{n_c}\frac{\mathrm{Re}\,\mu_n^2}{\mathrm{Im}\,\mu_n^2}. \tag{31}$$

The relation between the exact solution (19) and the latter formula has been analysed in [3]. This discussion will not be repeated here. Instead, relying on (31), we derive some approximate expressions for σ based on equivalent approximations of $\mathrm{Re}\,\mu_n^2$ and $\mathrm{Im}\,\mu_n^2$. In particular, the real part of μ_n^2 is sufficiently determined by $k_F^2 - (\kappa_n^0)^2$. In estimating the imaginary part, we make use of the approximate values for $-\mathrm{Im}\,\kappa_n^2$ and $\mathrm{Im}\,(\tilde{f}_v)_n$ given in section 5.

If we first restrict ourselves to very weak ($|\kappa_n^0\alpha| \ll 1$) surface roughness scattering, $\mathrm{Im}\,\mu_n^2 = -\mathrm{Im}\,\kappa_n^2$, and insert expression (25) into formula (31) we obtain

$$\sigma_s(d) \approx \frac{e^2k_F^4}{64\pi^7\hbar|\tilde{f}_s|^2\mathcal{N}_s S(n_c)}d^5\sum_{n=1}^{n_c}\frac{k_F^2 - n^2\pi^2/d^2}{n^2}. \tag{32}$$

Apart from different roughness parameters, this result agrees with the formula derived by Fishman and Calecki [2]. These authors employ the model of a continuously corrugated surface characterized by a root mean square height deviation Δ and a correlation length ξ. A comparison of formula (13) in the cited paper and (32) yields the reasonable interrelation $(4\pi|\tilde{f}_s|k_F^{-2})^2\mathcal{N}_s = V^2\mathcal{N}_s \approx \Delta^2\xi^2$ for the parameters used. As discussed in [2], the formula (32) predicts $\sigma_s \sim d^m$; m varies from $\leqslant 6$ if the first propagating mode has just been opened, to $\geqslant 2$ in the limit of a large number of propagating subbands $n_c \gg 1$. Indeed,

such a pronounced dependence on the film thickness has been confirmed by experimental investigations, cf the references in [2, 6].

While the properties of very thin films may be dominated by surface roughness, the general behaviour of σ is determined by both surface and volume scattering. Correspondingly, $\mathrm{Im}\,\mu_n^2$ comprises the volume term (30) as well as $-\mathrm{Im}\,\kappa_n^2$ as above. Equation (31) now yields

$$\sigma_{v,s}(d) \approx \sigma_b \frac{3}{2} \sum_{n=1}^{n_c} \frac{1 - n^2\pi^2/k_F^2 d^2}{(n_c + \frac{1}{2}) + (32\pi^5/k_F^4 d^5)|\tilde{f}_s|^2 \mathcal{N}_s S(n_c) n^2} \tag{33}$$

where we have introduced the bulk conductivity $\sigma_b = e^2 k_F^2 l/3\pi^2\hbar$. In the limit of large n_c, i.e. thick films $d > l$, the sum in the latter equation can be converted into an integral leading to

$$\frac{\sigma_{v,s}(d)}{\sigma_b} \approx 1 - \tfrac{32}{15}\pi |\tilde{f}_s|^2 \mathcal{N}_s \frac{l}{d} \tag{34}$$

i.e. only a small correction term of Fuchs–Sondheimer type [25, 26] remains from surface scattering. In the original Fuchs theory [25], surface roughness is characterized by a single phenomenological quantity, p, called the specularity parameter. The fraction of diffusely scattered particles, namely $(1 - p)$, is expressed in formula (34) in terms of the scattering cross-section, $\sim |\tilde{f}_s|^2$, and the density, $\mathcal{N}_s$, of surface scatterers. A detailed comparison yields

$$p = 1 - \tfrac{64}{45} 4\pi |\tilde{f}_s|^2 \mathcal{N}_s. \tag{35}$$

This relation can be conveniently used for a rough estimation of the strength of the surface scatterers considered.

The expressions (32)–(34) are based on the damping quantity (25), which requires a calculation of $\mathrm{Im}\,\tilde{f}_s$ via the optical theorem (5*b*). (Remember, however, that the finite value of $\mathrm{Im}\,\tilde{f}_s$ relies on the restriction to terms of the propagating modes only, cf (24).) This procedure has led to a rather strong dependence of σ on the thickness. Instead, we could consider $\mathrm{Im}\,\tilde{f}_s$ approximately as a constant parameter, i.e. independent of thickness. The corresponding roughness-induced damping quantity is given by (23). Inserting this expression into the conductivity (31), we obtain $\sigma_s \sim d^2$. This law represents a well known result discussed for instance in [1, 27]. The simultaneous occurrence of volume scattering leads again, in the limit of thick films, to a conductivity $\sigma_{v,s}$ of Fuchs–Sondheimer type, cf (34).

Up to the present point, we have used the limiting behaviour of $-\mathrm{Im}\,\kappa_n^2$ in the case $|\kappa_n^0\alpha| \ll 1$ (see section 5), i.e. when the lowest modes are only weakly influenced by surface roughness. For increasing surface scattering, the propagating subbands are eventually approximated better by expressions valid in the opposite limiting case $|\kappa_n^0\alpha| \gg 1$. The corresponding damping quantity is given by (26). Substituting $\mathrm{Im}\,\tilde{f}_s \approx k_0^3/8\pi^2\mathcal{N}_s^2$ from the optical theorem (28), it becomes $-\mathrm{Im}\,\kappa_n^2 \approx 2k_0(\pi\mathcal{N}_s h^2 d)^{-1}$. Now, the conductivity (31) yields

$$\sigma_{v,s}(d) \approx \frac{\sigma_b}{1 + 2l/\pi\mathcal{N}_s h^2 d}. \tag{36}$$

For dominating surface scattering ($l \gg d$), this formula asserts a weak dependence on the thickness, namely $\sigma_s \sim d$, whereas for thicker films or smaller mean free paths only a

correction of Fuchs–Sondheimer type arises from the roughness term in the denominator of (36). These results are in good agreement with measurements on ultrathin silver films published by Schad and co-workers [28]. Indeed, they have found that the conductivity of films after annealing follows a linear law $\sigma \sim d$ (d runs from a few monolayers to 125 monolayers). The conductivity of freshly deposited films rises significantly more slowly, however. This can be expected from the enhanced volume scattering (small l) due to growth defects. Due to annealing, these defects are partially removed leading to a considerable increase of the mean free path.

6.2. *Numerical results*

In the numerical calculations, the variable d and the parameters $co \equiv 4\pi|\tilde{f}_s|^2\mathcal{N}_s$, $\mathrm{Re}\,\tilde{f}_s$ and $l = (4\pi|\tilde{f}_v|^2\mathcal{N}_v)^{-1}$ are used. For the sake of brevity, all lengths are given in units of $\pi/k_0 = \pi/k_F = \lambda_F/2$. Half the Fermi wavelength is the period of oscillations due to the quantum size effect (QSE) and hence, in our context, the basic length scale of the system. The parameter co is a dimensionless quantity and can be associated with the extent to which the surface is effectively covered with scatterers. Additionally, in accordance with (32)–(34), the influence of surface scattering on the approximate conductivity is fixed by co. Via formula (35), this quantity can be expressed in terms of the more familiar specularity parameter.

In principle, our set of parameters could be completed by $\mathrm{Re}\,\tilde{f}_v$. However, the real part of $\tilde{f}_v(z)$ merely gives rise to a constant shift of $\mathrm{Re}\,\mu_n^2$ (8) which is omitted. So, the volume scattering processes are entirely determined by the mean free path l in agreement with other theoretical calculations and experimental studies.

In view of experimental investigations which have revealed QSE-induced oscillations of the conductivity [8–10], a parameter range of about $6.5 \lesssim l \lesssim 30$ seems to be of relevance. For good $CoSi_2$ films, larger values have been reported.

For $l \to \infty$, the properties of the physical quantities under consideration are solely influenced by surface roughness scattering. We start by focusing on this limiting case.

6.2.1. Surface scattering. Instead of the DOS itself (11), we have plotted in figure 2 the averaged DOS multiplied by d and normalized to the bulk DOS N_b. The resulting quantity is thus equal to the sum in (11), $\sum_{n=1}^{\infty} N_n$.

The curve for $co = \mathrm{Re}\,\tilde{f}_s = 0$ follows from N^0, see (13). In the ideal case, all propagating modes contribute the same portion to the total DOS, and every subband that becomes conducting increases the plotted quantity by one, leading to its staircase-like shape.

The further results shown in figure 2 reflect the influence of a finite surface roughness. The parameters are chosen such that $\mathrm{Im}\,\alpha \sim |\tilde{f}_s|^2$ is constant for all curves, whereas $\mathrm{Re}\,\alpha \sim co/\mathrm{Re}\,\tilde{f}_s$ varies. Accordingly the curves are shifted with respect to N^0. As can also be seen from figure 2, the broadening of the levels is less pronounced. The most significant changes appear in the vicinity of the subband thresholds. In particular, just below a threshold, the scattering into the lowest evanescent mode is enhanced leading to an increase of the corresponding DOS N_{n_c+1}. Just above a threshold, (12) predicts that the DOS of the highest propagating mode is reduced below the maximum value $N_{n_c} = 1$. These two mechanisms lead to the smooth shape of the DOS in figure 2, i.e. no discontinuities occur at the thresholds. Furthermore, it can be proved that increasing scattering processes, e.g. due to an increasing value of $\mathrm{Im}\,\alpha$ (not shown) or a finite value of l (see below), cause an enhanced smearing of the DOS.

In figure 2 the smearing of the DOS does not increase for a rising number of propagating modes contributing to intersubband transitions. This behaviour can be understood by bearing

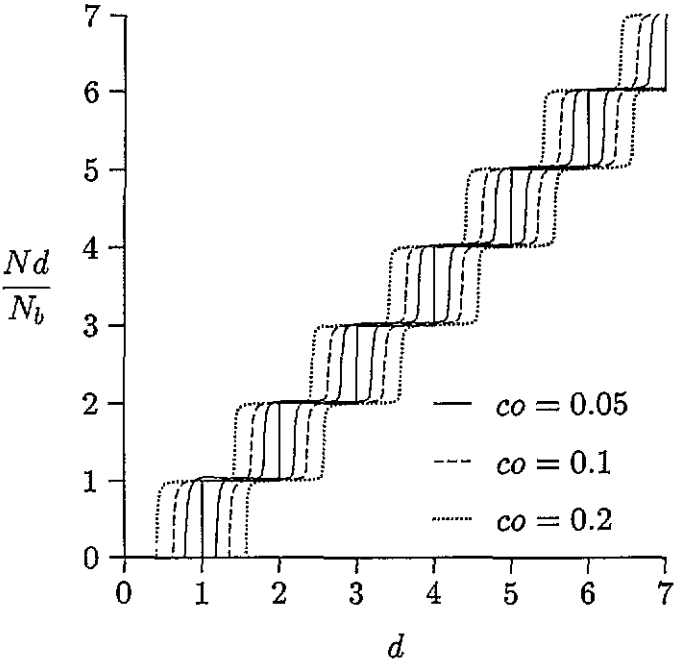

Figure 2. The laterally averaged DOS N (see (11)) multiplied by d/N_b as a function of the thickness d for three values of the parameter co and $\mathrm{Re}\,\tilde{f}_s = \pm 0.05$. For $\mathrm{Re}\,\tilde{f}_s \gtrless 0$, the thresholds are shifted to larger/smaller thicknesses, cf (21). The thicker full curve refers to a film with no scattering processes. (Remember that all lengths are given in units of π/k_F.)

in mind that a larger thickness (or n_c) is also accompanied by a reduction of the damping quantities $-\mathrm{Im}\,\kappa_n^2$, cf, for instance, (23).

In figure 3 the (reduced) conductivity (19) is shown for four sets of parameters taken from the figure of the DOS just discussed. As in figure 2, the shift of the different curves corresponding to different surface scatterers is obvious. In addition, we see that enhanced roughness scattering may lead to an increase of the conductivity, namely the dotted curve for $\mathrm{Re}\,\tilde{f}_s = 0.05$ and $co = 0.2$ lies above the full curve for the same $\mathrm{Re}\,\tilde{f}_s$ but a smaller value of co. To understand this result, remember that a larger value of $\mathrm{Re}\,\alpha \sim co/\mathrm{Re}\,\tilde{f}_s$ leads to a more pronounced shift of the subband thresholds to smaller energies, i.e. the in-plane energy increases. This behaviour is restricted, however, to very thin films. Indeed, for increasing d, the full curves rise faster than the dotted curves. This result is in agreement with the approximate expression (32) which asserts $\sigma_s(d) \sim co^{-1}$.

As can be seen from figure 3, a larger value of co is associated with a smaller amplitude of the quantum size oscillations. The smearing of these oscillations is weak, however, i.e. the conductivity retains a sawtooth-like shape which is a typical feature of calculations without level broadening. This result could be expected from the DOS, see figure 2, which is also only weakly rounded.

The influence of level broadening becomes more obvious if we compare the conductivity resulting from different $\mathrm{Im}\,\alpha \sim \mathrm{Im}\,\tilde{f}_s \sim |\tilde{f}_s|^2$, cf. the lower curves in figure 4. These results show clearly that σ behaves continuously at the thresholds and that the quantum size oscillations are smeared out. This qualitative behaviour of the conductivity can be explained in the same way as that of the DOS, see above. Just below a threshold σ is reduced due to the enhanced scattering into the lowest evanescent mode. Above a threshold the reduced

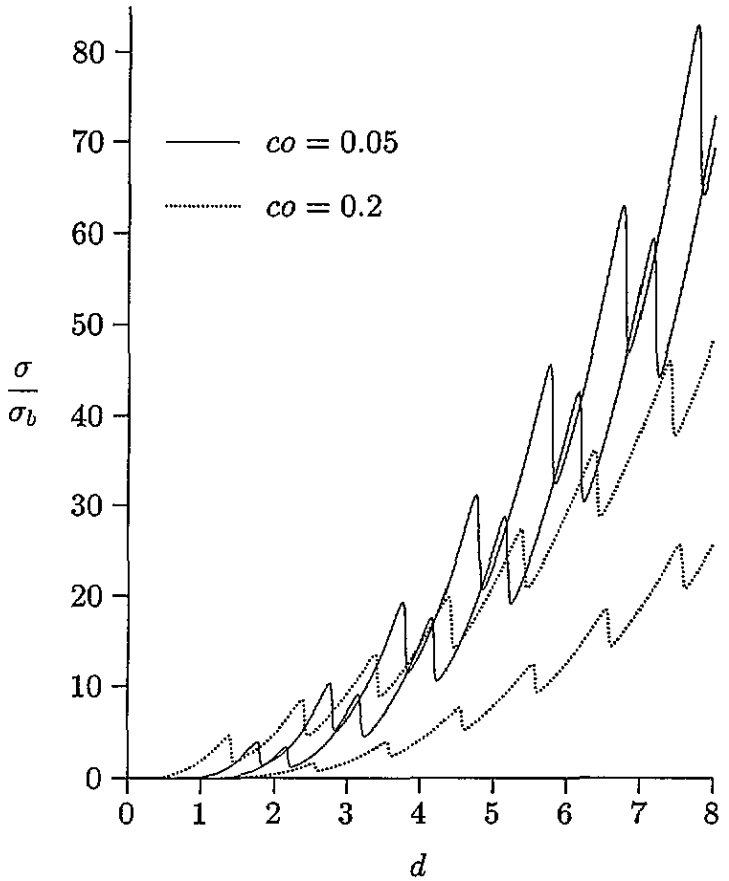

Figure 3. The reduced conductivity as a function of the thickness d for two values of the parameter co and $\mathrm{Re}\,\tilde{f}_s = \pm 0.05$. The bulk conductivity σ_b corresponds to a mean free path $l = 28.5$.

DOS of the highest propagating mode prevents this subband contributing significantly to the scattering of carriers occupying other modes. Remember that the intersubband transitions are weighted by the DOS of the final mode, see for example (29). As a consequence, σ drops below a conductivity calculated without level broadening.

In general, the density of scatterers $\mathcal{N}_s$ as well as $\mathrm{Re}\,\tilde{f}_s$, which is related to the volume of the individual surface irregularities (3), are a function of thickness and therefore should be derived from a growth model. In addition, different $\mathrm{Re}\,\tilde{f}_s$ can appear simultaneously. Our approach based on the SPM can be generalized to allow for such a more realistic description. Here, however, let us employ only a simple averaging procedure to reveal an effect which may result from different surface scatterers. In figure 4 the upper two curves represent mean values calculated from two solutions of σ referring to $\mathrm{Re}\,\tilde{f}_s = \pm 0.05$. Experimentally, this average corresponds to a layer evenly covered with sections of either bumps or dips. The result for $co = 0.2$ is derived from two largely shifted curves having almost coinciding thresholds. This implies that it agrees roughly with the conductivity of a film with one type of scatterer only. It is more likely, of course, that the superposition of two original curves yields a mean conductivity as that referring to $co = 0.05$ (see figure 4, uppermost curve). The peaks of this curve are almost equidistant, pretending that the period

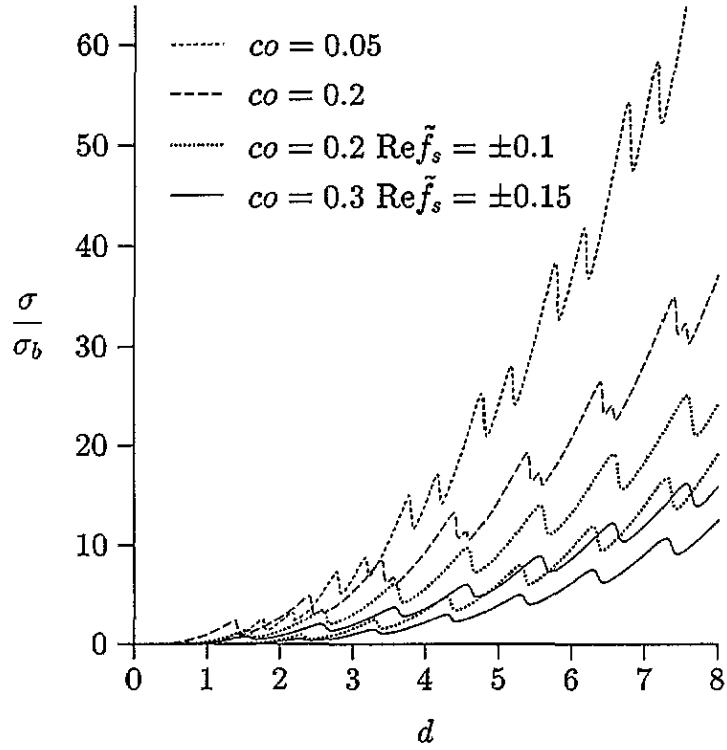

Figure 4. The reduced conductivity as a function of the thickness d. The upper two curves represent averaged values which are calculated from two results for $\mathrm{Re}\,\tilde{f}_s = 0.05$ and $\mathrm{Re}\,\tilde{f}_s = -0.05$, respectively. The lower four curves have equal values of $|\mathrm{Re}\,\alpha|$ but differ with respect to $\mathrm{Im}\,\alpha$. (The curves for positive (negative) $\mathrm{Re}\,\tilde{f}_s$ are shifted to smaller (larger) thicknesses.) The bulk conductivity σ_b corresponds to a mean free path $l = 28.5$.

of the quantum size oscillations is half as small as it should be. One can imagine that the superposition of more than two types of scatterer can give rise to further fictitious periods.

6.2.2. Surface and volume scattering. In figure 5 the DOS is shown for different parameters. For a decreasing mean free path and/or a larger number of propagating modes, the steps of the ideal DOS N^0 (13) are washed out and finally disappear. This is reasonable, in view of the arguments given above. Similarly, the conductivity plotted in figure 6 exhibits a more pronounced smearing caused by the self-consistent level broadening. (To avoid misunderstanding, we point out that the conductivity σ for the parameter l is given in units of $\sigma_b \sim l$.) It is worth mentioning, however, that the position of the thresholds depends on the choice of the parameter l, too. In particular, the maximum conductivities are shifted to smaller d for decreasing values of l, whereas the location of the corresponding minima is almost unchanged. Thus, not only surface scattering but also volume scattering (along with a non-zero surface roughness) gives rise to a shift of the oscillations in the conductivity.

Finally, in figure 7 we have shown averaged conductivities and a result following from volume scattering only. In accordance with the increase of the total scattering processes, the full curve lies below the upper broken curve. In addition, the amplitude of the QSE-induced oscillations is considerably reduced due to the enhanced level broadening and the occurrence of different types of scatterer. The general shape of the full curve is in good agreement with experimental results on ultrathin films.

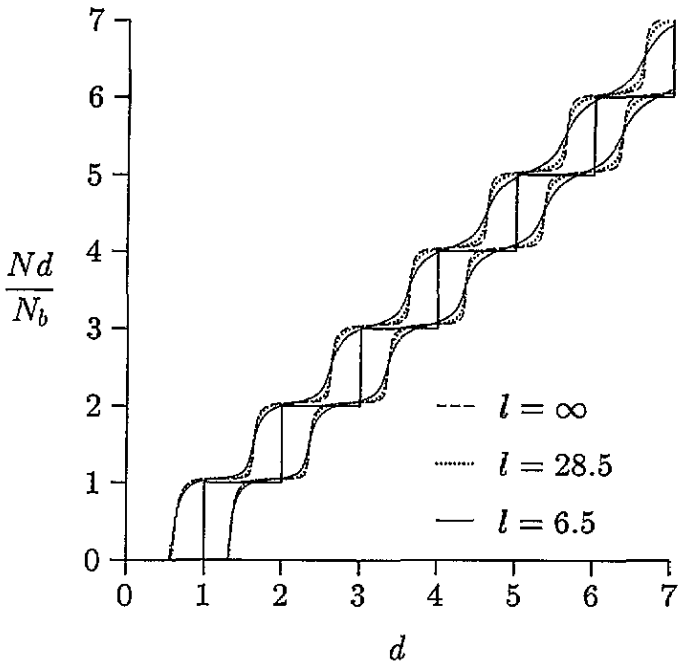

Figure 5. The laterally averaged DOS N (see (11)) multiplied by d/N_b as a function of the thickness d for three values of the mean free path l and a roughness fixed by $co = 0.2$ and $\mathrm{Re}\,\tilde{f}_s = \pm 0.1$. For $\mathrm{Re}\,\tilde{f}_s \gtrless 0$, the thresholds are shifted to larger/smaller values of d. The thicker full curve refers to a film with no scattering processes at all, i.e. $co = \mathrm{Re}\,\tilde{f}_s = l^{-1} = 0$.

7. Summary

From the very beginning, the quantum mechanical description of thin films has been based on the concept of lateral subbands. This implies that a sound evaluation of all quantities is required that characterize these subbands. In this paper, we have put forward a theory that enables us to determine self-consistently the scattering-induced broadening of the levels. The basic formulae employed in our approach are the equations for the Green function G and two optical theorems with respect to volume and surface scatterers, respectively. As usual, volume scattering appears directly as a damping term in the differential equation for G. To incorporate surface scattering, however, we have derived a complex boundary condition (2*b*) imposed on G. For vanishing volume scattering, the Green function is diagonal with respect to a lateral mode representation and, in principle, can be found for any roughness parameter α, where $\alpha = 4\pi \tilde{f}_s \mathcal{N}_s$ determines completely the surface properties in the boundary condition. The appearance of diagonal elements only in G is due to the fact that for each thickness d and each surface roughness α a specific set of adapted eigenfunctions is calculated. In this sense, our approach contrasts with the familiar perturbational treatment of surface roughness. There, transition matrix elements are evaluated based on the unperturbed eigenfunctions of a smooth film. For increasing roughness and, consequently, increasing matrix elements the theory becomes inappropriate.

The boundary condition leads to some interesting features of the complex lateral eigenvalues κ_n. (Remember that $\kappa_n^0 = n\pi/d$, $n = 1, 2, \ldots$, for a smooth film.) Firstly, the real part moves for higher n values from an integer multiple of π/d to the next larger or smaller one, depending on the sign of $\mathrm{Re}\,\alpha$, when n goes from one

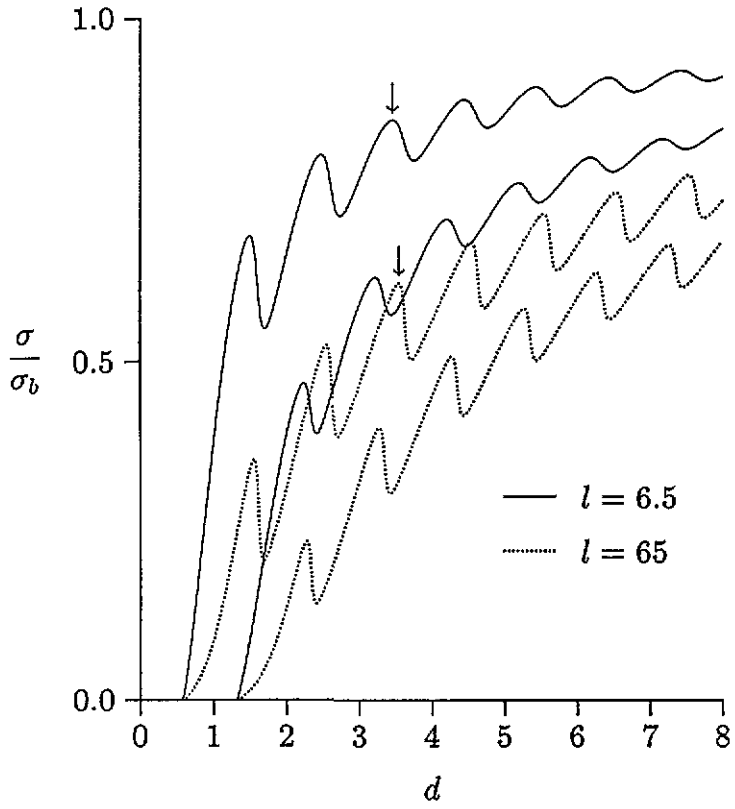

Figure 6. The reduced conductivity as a function of the thickness d for two values of the mean free path l. The surface roughness is determined by $co = 0.2$ and $\mathrm{Re}\, \tilde{f}_s = \pm 0.1$. (The curves for $\mathrm{Re}\, \tilde{f}_s > 0$ start at smaller values of d.) The arrows indicate that the thresholds are slightly shifted. The bulk conductivity σ_b refers to the value of the mean free path l used in the calculation of the corresponding σ.

to infinity. Secondly, the imaginary part (or, strictly speaking, $|\mathrm{Im}\, \kappa_n|$) associated with roughness-induced intersubband transitions increases linearly with n, passes a maximum and approaches zero again as n^{-1}, $n \to \infty$. Only the linear regime leading to $-\mathrm{Im}\, \kappa_n^2 \sim n^2$, see (23), is related to the results derived from perturbational calculations. Nevertheless the whole behaviour is readily understood in terms of scattering theory. Indeed, if we assign a wavelength $\lambda_n \sim (\mathrm{Re}\, \kappa_n)^{-1}$ to each individual mode, the strongest scattering (i.e. maximum $|\mathrm{Im}\, \kappa_n|$) of a wave incident on the surface occurs if λ_n is comparable with the size $\sim h = \mathrm{Re}\, \alpha$ of surface irregularities. For $\lambda_n \gg h$, which may be satisfied for the lowest modes, the incident wave does not resolve the rough shape of the surface and thus $|\mathrm{Im}\, \kappa_n|$ is small. In the opposite case, $\lambda_n \ll h$, we are again guided by these considerations to a small value of $|\mathrm{Im}\, \kappa_n|$. On principle, the discussed properties of both the real and imaginary parts of the lateral eigenvalues are essential, for example to make convergent the sum in the optical theorem (5*b*) for the surface scatterers.

As shown in sections 5 and 6, the reproduction of standard results deduced within the scope of perturbational methods relies on the neglect of level broadening and the use of κ_n in the linear regime mentioned above. The existence of eigenvalues of this kind is associated with the condition $|\alpha \kappa_n^0| = n\pi h/d \ll 1$ (21) being fulfilled for a sufficiently large number of n. Thus, such a region has not necessarily to exist. On the other hand,

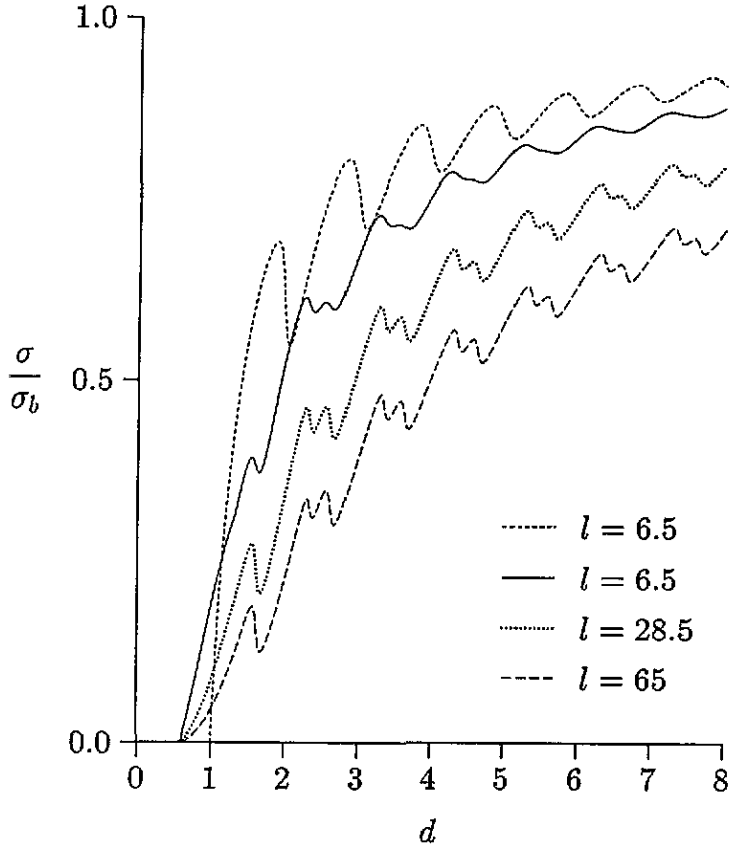

Figure 7. The reduced conductivity as a function of the thickness d. The uppermost curve corresponds to the occurrence of volume scattering processes only, i.e. $co = \mathrm{Re}\,\tilde{f}_s = 0$. The others represent averaged values which are calculated from two results for $\mathrm{Re}\,\tilde{f}_s = 0.05$ and $\mathrm{Re}\,\tilde{f}_s = -0.05$, respectively, and $co = 0.2$. As in figure 6, the bulk conductivity σ_b refers to the value of the mean free path l used in the calculation of the corresponding σ.

using the eigenvalues of the opposite limiting case $|\alpha\kappa_n^0| \gg 1$, we have derived an analytical expression for σ (see (36)) and shown that measurements are well described by applying this theoretical result.

In view of experimental investigations our approach described here is mainly limited due to the consideration of only one type of surface scatterer, independent of thickness. (Of course, the latter restriction corresponds to the assumption of a thickness-independent correlation function in the model of a continuously corrugated surface usually made by other authors.) These restrictions are not a matter of principle. While the inclusion of further kinds of (surface) scatterer is straightforward in the framework of the SPM, the use of thickness-dependent surface parameters requires additional effort (e.g. a growth model). Calculations along these lines will be left for the future. Nevertheless, our present theory already yields some results that are interesting from an experimental point of view. (1) Scattering-induced level broadening suppresses the QSE oscillations. As well as a macroscopically varying thickness that averages out all discrete features [1], level broadening can account for the fact that the usually predicted oscillatory behaviour of the conductivity and other physical quantities is less clearly seen in experiment. (2) According to our calculations (see section 6)

surface as well as volume scattering gives rise to a parameter-specific shift of the thresholds as a function of d [29]. This may explain why differently deposited layers exhibit quantum size oscillations which are slightly shifted against each other [10, 30]. (3) We have shown that the appearance of different types of surface scatterer (bumps and dips), even in a rather simple model, can lead to additional quantum size-induced peaks in the conductivity (or steps in the DOS) and a loss of the original period $\lambda_F/2$. Instead of $\lambda_F/2$, a number of fictitious periods can occur and complicate the interpretation of experimental data. These effects may also account for an unsuccessful search for quantum size oscillations [11].

Acknowledgments

I wish to thank Professor M Jalochowski for valuable conversations on the experimental investigation of thin films and Professor R Lenk for many fruitful discussions throughout the course of this work. In addition, I am grateful to Dr D Mirschinka for comments on the mathematical problems associated with the boundary condition.

References

[1] Trivedi N and Ashcroft N W 1988 *Phys. Rev.* B **38** 12298
[2] Fishman G and Calecki D 1989 *Phys. Rev. Lett.* **62** 1302
[3] Knäbchen A 1995 *Thin Solid Films* to be published
[4] Levinson Y B and Sukhorukov E V 1991 *Phys. Lett.* **149A** 167
[5] Kunze C 1993 *Phys. Rev.* B **48** 14338
[6] Kunze C 1993 *Solid State Commun.* **87** 359
[7] Hoffmann H and Fischer G 1976 *Thin Solid Films* **36** 25
[8] Fischer G and Hoffmann H 1980 *Solid State Commun.* **35** 793
[9] Jalochowski M and Bauer E 1988 *Phys. Rev.* B **38** 5272
[10] Jalochowski M, Bauer E, Knoppe H and Lilienkamp G 1992 *Phys. Rev.* B **45** 13607
[11] Badoz P A, Arnaud d'Avitaya F and Rosencher E 1991 *Ann. Phys., Paris* **16** 623
[12] Sandomirskii V B 1967 *Zh. Eksp. Teor. Fiz.* **52** 158 (Engl. transl. 1967 *Sov. Phys.–JETP* **25** 101)
[13] Leung K M 1984 *Phys. Rev.* B **30** 647
[14] Tešanović Z, Jarić M V and Maekava S 1986 *Phys. Rev. Lett.* **57** 2760
[15] Fishman G and Calecki D 1991 *Phys. Rev.* B **43** 11581
[16] Meyerovich A E and Stepaniants S 1994 *Phys. Rev. Lett.* **73** 316
[17] Lenk R 1990 *Phys. Status Solidi* b **162** 227
[18] Lenk R 1991 *Solid State Commun.* **79** 531
[19] Knäbchen A 1992 *Phys. Rev.* B **45** 8542
[20] Lenk R 1990 *Phys. Status Solidi* b **161** 797
[21] Voronovich A G 1994 *Wave Scattering from Rough Surfaces (Springer Series on Wave Phenomena 17)* (Berlin: Springer)
[22] Ogilvy J A 1987 *Rep. Prog. Phys.* **50** 1553
[23] Ryshik I M and Gradstein I S 1957 *Tables of Series, Products, and Integrals* (Berlin: Deutscher Verlag der Wissenschaften)
[24] Dunford N and Schwartz J T 1974 *Linear Operators (vol III: Spectral Operators)* (Moscow: Mir)
[25] Fuchs K 1938 *Proc. Cambridge Phil. Soc.* **34** 100
[26] Sondheimer E H 1952 *Adv. Phys.* **1** 1
[27] Knäbchen A 1995 *J. Phys.: Condens. Matter* **7** 55
[28] Schad R, Heun S, Heidenblut T and Henzler M 1992 *Phys. Rev.* B **45** 11430
[29] Lee E Y, Sirringhaus H and von Känel H 1994 *Phys. Rev.* B **50** 5807
[30] Jalochowski M 1994 private communication